Available online at www.sciencedirect.com

SCIENCE DIRECT®

Cement and Concrete Research 35 (2005) 1391 – 1399

Cement and Concrete Research

An experimental study on corrosion resistance of concrete with ground granulate blast-furnace slag

Kyong Yun Yeau[a,*], Eun Kyum Kim[b]

[a]*School of Civil and Environmental Engineering, Yonsei University, Seoul, Republic of Korea*
[b]*Dept. of Civil Engineering, Seoul National Univ. of Technology, Seoul, Republic of Korea*

Received 28 April 2004; accepted 11 November 2004

Abstract

This paper presents experimental test results on corrosion resistance of concrete containing ground granulate blast-furnace slag (GGBS) and ASTM Type I or ASTM Type V cement. To investigate the problem, a series of tests were performed. First, rapid chloride permeability tests were executed in accordance with ASTM C 1202 to determine the qualitative terms of chloride-ion penetrability. Second, accelerated chloride-ion diffusion tests were done to calculate diffusion coefficients of chloride-ions permeated through concrete specimens. Third, accelerated steel corrosion tests were carried out by using the repeated wetting and drying technique. Fourth, half-cell potential tests were implemented in accordance with ASTM C 876 to evaluate the probability of steel corrosion. Finally, the surface area of corrosion on embedded steel in concrete specimens was measured to confirm half-cell test results. Test results showed that the coefficient of permeability of Type I cement concrete was lower than that of Type V cement concrete. All the concrete mixed with GGBS exhibited lower diffusion coefficient, compared to GGBS-free concrete. Moreover, the corrosion probability of steel bar in Type V cement concrete was higher than that of steel bar in Type I cement concrete. Based on the test results, it is suggested that much stronger corrosion resistance can be achieved, if higher volume of GGBS is added in Type I cement rather than Type V cement.

© 2004 Elsevier Ltd. All rights reserved.

Keywords: Corrosion resistance; Ground granulate blast-furnace slag; ASTM Type I and ASTM Type V cement

1. Introduction

High quality and durable concrete is required to reduce the rapid deterioration of concrete in severe conditions. Among the factors related to declining concrete durability such as carbonation, corrosion, alkali–silica reaction, freezing/thawing, and so on, the penetration of chloride-ions into concrete has been regarded as the major deterioration problem. Ingress of chloride-ions destroys the natural passivity of the surface of reinforcing steel, and often leads to the corrosion of steel in concrete structures. Thus, insufficient concrete cover or poor quality concrete accelerates reinforcement corrosion. Particularly, environmental conditions in offshore or coastal region reduce useful service-life of concrete structures due to chloride-ion attacks. Previous studies [1–5] have shown that use of cement replacement materials such as fly ash, silica fume, blast-furnace slag, etc. may reduce greatly the probability of steel corrosion as well as the permeability of concrete. Especially, silica fume is known to considerably increase the durability of concrete. However, its cost is so high and its workability is so low that fly ash and/or slag are widely used as substitutes in Korea. Torii [6] reported that resistance to chloride penetration of 50% ground granulated blast-furnace slag (GGBS) concrete was almost the same as that of 10% silica fume concrete.

Recently, offshore, coastal, and marine concrete structures were constructed in Korea from GGBS concrete because high volume of GGBS can contribute to the reduction of chloride ingress. Most of GGBS used were also blended with American Society of Testing Materials (ASTM) Type V sulfate-resistant cement rather than ASTM Type I Portland cement, in order to protect the constructed

---

* Corresponding author. Fax: +82 2 948 0043.
E-mail address: ky_yeau@hotmail.com (K.Y. Yeau).

0008-8846/$ - see front matter © 2004 Elsevier Ltd. All rights reserved.
doi:10.1016/j.cemconres.2004.11.010

Table 1
Chemical compositions and physical properties of cement and GGBS used

Chemical compositions (%)	Type I cement	Type V cement	GGBS
Silicon dioxide, SiO_2	21.0	22.7	33.31
Aluminum oxide, Al_2O_3	5.9	4.1	14.60
Ferric oxide, Fe_2O_3	3.2	4.4	0.4
Calcium oxide, CaO	62.5	62.7	41.63
Magnesium oxide, MgO	3.02	2.54	7.21
Sodium oxide, Na_2O	0.12	0.09	0.164
Potassium oxide, K_2O	0.78	0.59	0.316
Sulfur trioxide, SO_3	2.1	1.8	–
Sulfur dioxide, SO_2	–	–	0.034
Sulfur, S	–	–	0.82
Titanium dioxide, TiO_2	–	–	1.4
Chlorine, Cl	–	–	0.006
Loss on ignition	1.61	1.40	
Potential mineral composition (%)			
C_3S	44.64	43.76	–
C_2S	26.53	32.07	–
C_4AF	9.74	13.39	–
C_3A	10.22	3.42	–
Physical properties of cement and GGBS			
Special gravity	3.15	3.15	2.92
Fineness (cm^2/g)	3200	3250	4000

structures from sulfate attack. Although Type V cement can increase the chemical resistance to the sulfate attack that causes expansion and cracking of concrete [7], corrosion resistance of reinforcement in concrete is aggravated, because the tri-calcium aluminate (C_3A) contents of Type V cement is much lower than those of Type I cement. The C_3A phase of the Type I cement plays a dominant role in binding the chloride-ions [8]. Hussain [9] reported that the chloride binding capacity and reinforcement corrosion initiation time can be increased by 2.43 and 2.45 folds, respectively, in accordance with increase of C_3A content from 2% to 14%. Rasheeduzzafar [10] found that Type I cement containing 9.5% C_3A by weight binds almost 1.6 times more chloride than the cement that contains 2.8%, and thus, Suryavanshi [11] suggested that cement containing abundant C_3A phase is recommended for structure in coastal and marine environments. Dehwah [12] indicated that the presence of sulfate ions in chloride environments did not affect the time-to-initiation of reinforcement corrosion. Therefore, it can be concluded that protecting the ingress of chloride-ions is more useful than preventing the attack of sulfate ions in case of the coexistence of sulfate and chloride-ions.

In this study, corrosion resistance was evaluated for two Types of Portland cement, mixed with GGBS varying 0 to 50% in content contribution. Based on the test results, permeability, diffusivity, corrosion potential, and surface area of steel corrosion were measured. Results from respective cases were, then, compared to assess the variation of the corrosion resistance among several types of concrete.

2. Experimental program

Two types of cement, Type I cement and Type V cement, were used throughout this work. Cement replacement, ground granulated blast-furnace slag, was also used. Table 1 presents test data of chemical compositions and physical properties of GGBS and cement. Sea sand and crushed sand were used as fine aggregate. Crushed limestone was used as coarse aggregate. Melamine-based superplasticizer satisfied with the ASTM C 494 [13] requirements was used to obtain desired workability.

2.1. Materials and mix proportions

Four types of different mixtures were proportioned, and designated as B1, B2, B3, and B4 as shown in Table 2. Mixture B1 containing only cement was used as a control mixture. These concrete mixtures were proportioned to have the 28-day strength of 35 MPa. Additionally, the other mixtures, B2, B3, and B4, were proportioned to have cement replacements in the range of 25% to 55% by weight of cement. Slump of 15 cm was maintained. These mixtures were proportioned for water-to-binder ratio of 41.8%. Moreover, two different types of cement, Type I cement and Type V cement, were used for a comparison of corrosion resistance effects.

2.2. Specimen preparation and testing

2.2.1. Compressive test

100 mm×200 mm concrete cylinders were tested in compression at 7, 14, 28, and 56 days. All specimens for compression test were capped with sulfur compound before testing.

Table 2
Concrete mixture design

Mixture no.	B1 (0% GGBS)	B2 (25% GGBS)	B3 (40% GGBS)	B4 (55% GGBS)
Cement, kg/m^3	385	289	231	173
GGBS, kg/m^3	0	96	154	212
Water, kg/m^3	161	161	161	161
Water to binder ratio, %	41.8	41.8	41.8	41.8
Sea sand, kg/m^3	573	573	573	573
Crushed sand, kg/m^3	247	247	247	247
Crushed coarse aggregate, kg/m^3	977	977	977	977
Sand to aggregate Ratio, %	46	46	46	46
Superplasticizer, kg/m^3	1.60 (1.70)	1.60 (1.20)	1.55 (1.70)	1.60 (1.20)
Slump, mm	150	150	150	150
Concrete density, kg/m^3	2345	2345	2345	2345

Note: ( ) means the amount of superplasticizer used in Type V cement.

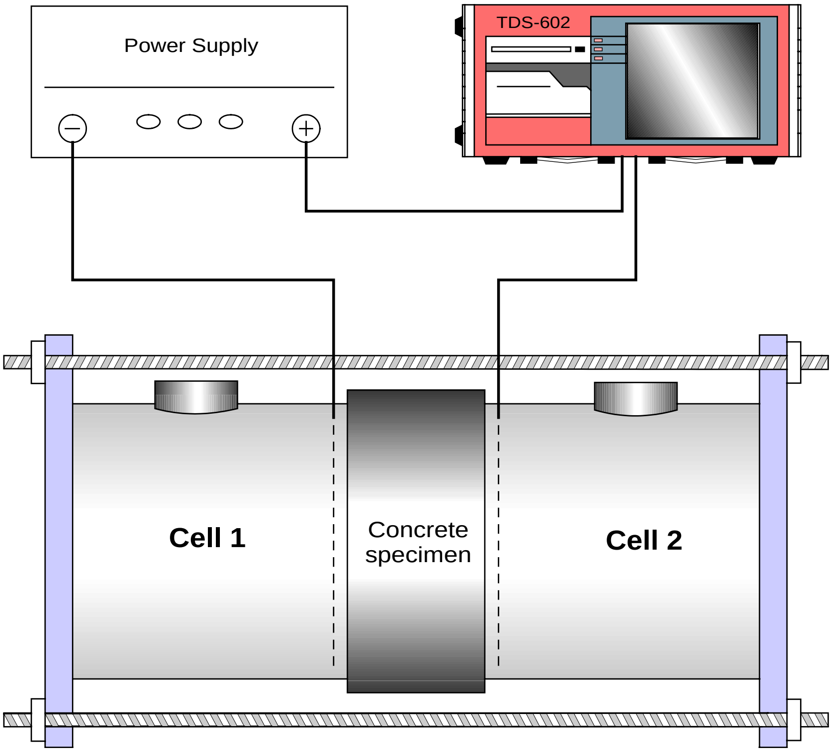

Fig. 1. Schematic view of diffusion cell and experimental set-up.

2.2.2. Rapid chloride permeability (RCP) test

The method of RCP test designated in ASTM C 1202-97 [14] was adopted in this study. The whole test configuration is shown in Fig. 1. The amount of charge passed through the concrete specimen, as an electrical indication of chloride permeability, is monitored during a 6-h test duration. After 28-days or 56-days curing, the 100 mm×200 mm concrete cylinders were sliced into 50 mm thick sections, and then into 25 mm, parts of each cylinder were trimmed and discarded. Center section among three 50 mm sections is used in test. The concrete specimen is assembled with two applied diffusion cells. During the test, a potential difference of 60 V DC is maintained across the diffusion cells. The upstream cell (cathode) is filled with 5% sodium chloride (NaCl) solution, and the downstream one (anode) is filled with saturated calcium hydroxide solution.

2.2.3. Accelerated chloride-ion diffusion (ACID) test

The ACID test was used to determine the diffusion coefficients of chloride-ions passed through concrete speci-

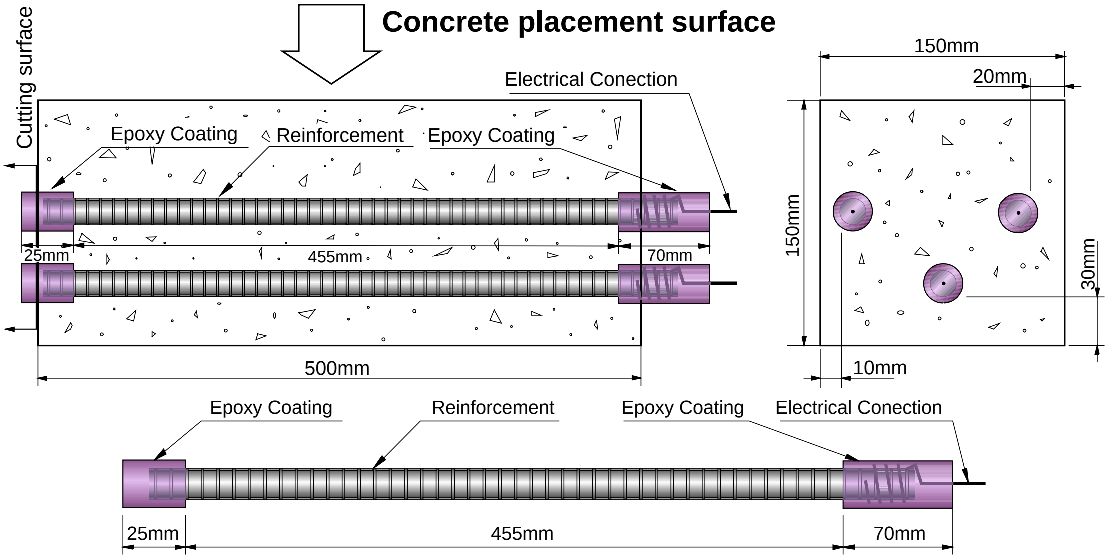

Fig. 2. Reinforcing steel bar layout of concrete specimen.

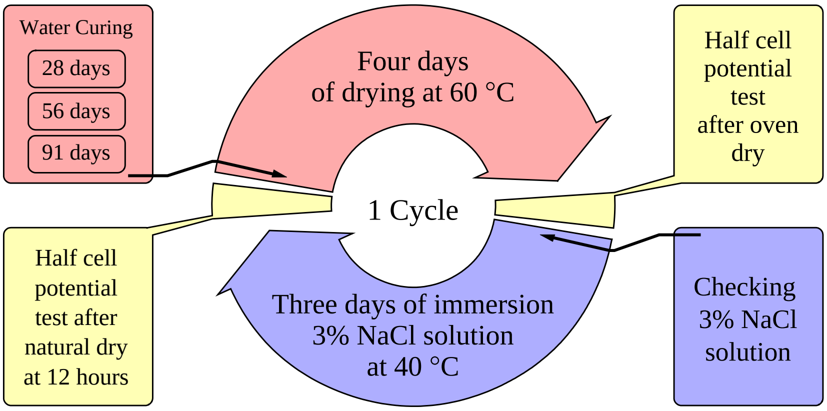

Fig. 3. Cycle routine for accelerating corrosion of steel in concrete specimen.

mens. This test modified the rapid chloride permeability test of ASTM C 1202. Experimental procedures were the same as ASTM C 1202 except for voltage and test duration. The tests were conducted after the specimens are cured in water for 7, 14, and 28 days. In order to accelerate the diffusion rate of chloride-ions, a potential difference of 30 V DC was applied to the electrodes [15]. Dhir and Sugiyama's equation (Eq. (1)) was used to calculate chloride diffusion coefficient [16,17].

$$D_{\mathrm{Cl}} = \frac{RT}{Z_{\mathrm{Cl}} F C_{\mathrm{Cl}}} \frac{l}{\Delta E} \frac{V}{A} \frac{\mathrm{dC}}{\mathrm{dt}} \left(\mathrm{cm}^2/\mathrm{s}\right) \tag{1}$$

where, D_{Cl} (cm^2/s)=diffusion coefficient, R=universal gas constant (8.314 J/mol K), T=absolute temperature (K), Z_{Cl}=electrical charge, F=Faraday constant (96,485 J/V mol), C_{Cl}=chloride concentration of cathode (mol/l), l=specimen thickness (cm), ΔE=potential difference (V), V=volume of diffusion cell (l), A=specimen area (cm^2), dC=chloride concentration of diffusion cell (mol/l), and dt=elapsed time (s).

2.2.4. Accelerated steel corrosion (ASC) test

The ASC test was conducted to measure half-cell potential and the surface areas of steel bars corroded. For the test, 150×150×500 mm concrete specimens were prepared as shown in Fig. 2. The specimens have three different concrete covers, 10, 20, and 30 mm. The repeated wetting and drying method described in Fig. 3 was used to accelerate steel corrosion. After curing the concrete specimens in water for three different days, 28 days, 56 days, and 91 days, these tests were conducted up to 30 cycles. For each wetting–drying cycle, test specimens were wetted in 3% NaCl solution for 3 days and then dried at 60 °C for 4 days. After 30 weeks, the specimens were crushed out and the surface area corroded was calculated as a percentage to the total area of steel embedded in concrete.

Table 3
Estimate of corrosion on half-cell potential test

Potential (mV)	Probability of the presence of active corrosion
>−200	Very high probability over 90% of no corrosion
−200~−350	Uncertain
<−350	Very high probability over 90% of corrosion

2.2.5. Half-cell potential (HP) test

HP measurements give an indication of the corrosion risk of steel and are linked to the empirical probability of corrosion suggested by Kostogloudis [18]. The measurements were performed by using a CSE (Copper–copper Sulfate Electrode) at the end of every cycle according to ASTM C 876-99 [19]. ASTM C 876 suggests the estimation criterion of corrosion according to the range of the half-cell potential as shown Table 3.

3. Results and discussions

3.1. Compressive strength

The compressive strength data of Type I cement are shown in Fig. 4. At the 14-day age, all the concrete mixture

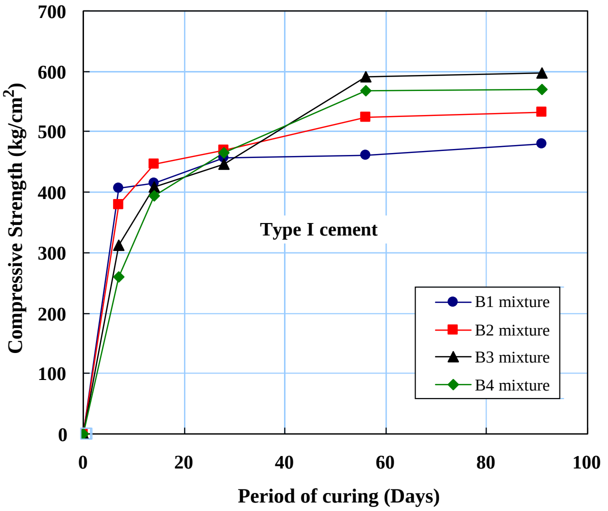

Fig. 4. Compressive strength versus curing period of specimens blended with Type I cement and GGBS of 0, 25, 40, and 55% by binder weight, respectively.

specimens made with or without ground granulate blast-furnace slag (GGBS) showed strengths in excess of 350 kg/cm^2. The performances of the GGBS-containing mixtures (B2, B3, and B4) were similar to that of the B1 mixture at 28 days, but were superior to that of the B1 mixture at 56 days. At the early age before 7 days, all the GGBS mixtures, up to 55% cement replacement, attained lower compressive strengths than the B1 mixture. These results suggested that latent hydraulicity reactions by GGBS slowed down the development of compressive strength with an increase in GGBS content at the early age. However, at later times, 28, 56, and 91 days, the compressive strengths of the GGBS concrete mixtures were similar or slightly stronger than that of GGBS-free concrete (B1).

Fig. 5 presents the compressive strength data of Type V cement for all GGBS mixtures. The strength-development of Type V cement was similar to that of Type I cement. The short-term strength of the GGBS mixtures before 28 days was also weaker than that of the GGBS-free mixture. GGBS concrete mixtures showed similar or slightly higher strength development, compared to B1 concrete mixtures at 28 days.

3.2. Chloride permeability characteristics

All concrete mixtures were evaluated for resistance to chloride-ion penetration according to the RCP test designated in ASTM C 1202-97. The RCP test data for Type I cement and Type V cement are presented in Fig. 6. These tests were carried out for all concrete mixture specimens after curing in water at 28 and 56 days. In general, the chloride penetration of concrete decreased with an increase in curing period. All concrete specimens with GGBS cement exhibited lower chloride penetration compared to the B1 concrete mixture. The difference was remarkable as the period of curing and GGBS content, especially 40% and 55% content, were increased. Chloride-ion penetrability based on charge passed gradually decreased with an increase in GGBS content. Hussain [20] and Kumar [21] indicated that the average pore size of ordinary Portland cement concrete was 1.57–2 times larger than that of GGBS concrete because the latent hydraulicity reaction of GGBS does not only make the cement matrix more dense but also diminishes the pore size. The small pore size decreases the penetration and diffusion of chloride-ions. In this study, the results arise from the fact that the latent hydraulicity reactions of GGBS make the microstructure of the specimens denser. Therefore, the permeability becomes lower in accordance with the addition of higher volumes of GGBS.

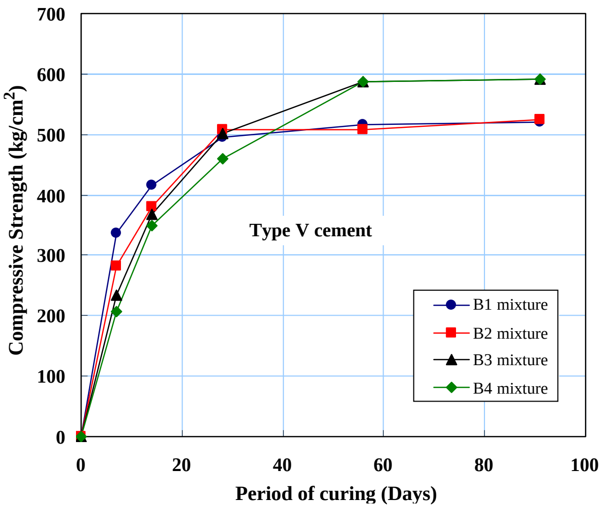

Fig. 5. Compressive strength versus curing period of specimens blended with Type V cement and GGBS of 0, 25, 40, and 55% by binder weight, respectively.

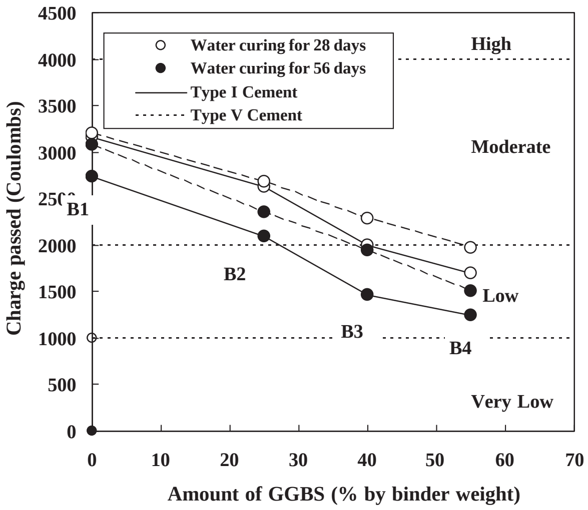

Fig. 6. Rapid chloride permeability of specimens with GGBS.

B3 mixtures blended with Type I cement received ratings varying from “moderate” at 28 days to “low” at 56 days, according to the chloride-ion penetrability recommended by ASTM C 1202. The penetration of B4 mixture specimens was recorded at “low” levels, but B1 and B2 mixtures still stayed at “moderate” level penetration at 28 days and 56 days, respectively. In the case of Type V cement, B4 mixtures closely reached “low” grades at 28 days. These results suggest that at up to 40%, Type V cement can be replaced with GGBS without any negative effects and concrete resistance to chloride-ion penetration slightly improved. It also indicates that the permeability of Type I cement blended with GGBS is lower than that of Type V cement.

3.3. Evaluation of chloride-ion diffusion coefficient

Figs. 7 and 8 show the ACID test results obtained from the cumulative increase of chloride-ion concentration passing the concrete specimens that were cured in water for 28 days. The relationship between the concentrations of chloride-ions versus elapsed time can represent a straight line; a flat line, representing transition periods; and a sloped line, which is termed as steady-state periods or flux. According to the increase in GGBS content, the transition

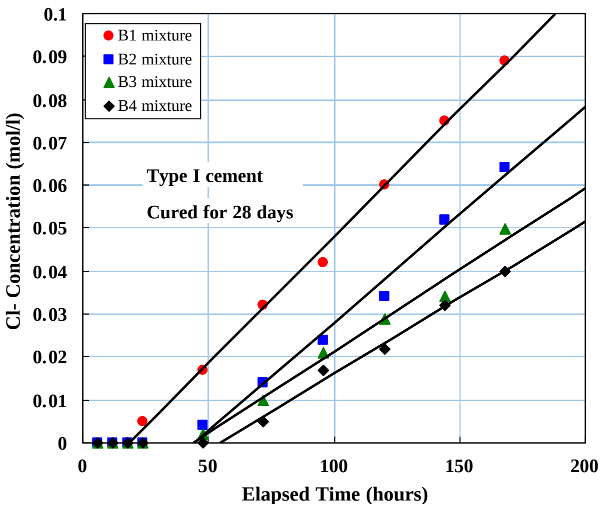

Fig. 7. Cumulative increase in chloride-ion concentration of Type I cement.

periods, the elapsed time in which chloride-ions penetrate the specimens, were increased and the slopes of the steady-state periods were decreased. These results indicate that much longer transition periods and much lower chloride-ion concentration can be achieved, if higher volumes of GGBS are added. In the case of Type V cement concrete, the ACID test results, as shown in Fig. 8, indicate similar results as the ACID test of Type I cement concrete. However, the chloride-ion concentrations of Type I cement are lower than that of Type V cement given the same amount of GGBS.

From the above results, the diffusion coefficients of chloride-ions in concrete mixed with GGBS were calculated by Eq. (1). The calculated results are shown in Fig. 9. Diffusion coefficients were decreased in accordance with an increase in GGBS content and the period of curing. Type I cement showed a lower diffusion coefficient compared to Type V cement. In particular, the diffusion coefficient of the B4 mixture was about one-third smaller than that of the B1 mixture. Rasheeduzzafar [22] and Suryavanshi [23] evaluated the effects of reducing the free chloride-ion content in concrete by increasing the tri-calcium aluminate (C_3A) content. Their results showed that the amount of binding chloride-ions increased as C_3A content was increased. In addition, the diffusion coefficient decreased with an increase in C_3A content due to increasing binding chloride-ions. Thus, the results of this test indicate that the diffusion coefficient of Type I cement concrete is lower than that of Type V cement concrete. Moreover, the diffusion coefficient of concrete decreased as the amount of GGBS was increased.

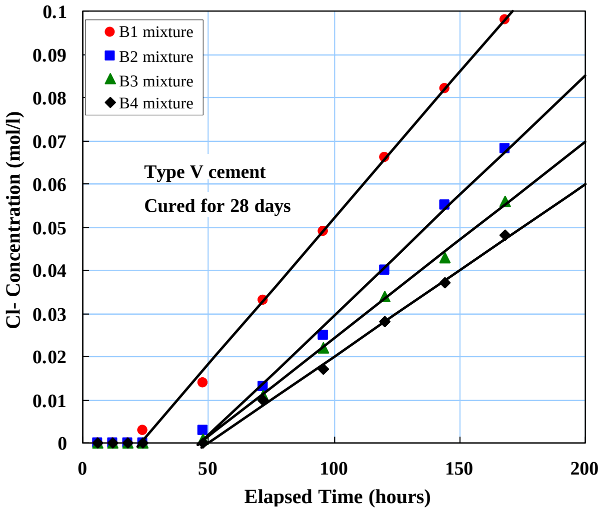

Fig. 8. Cumulative increase in chloride-ion concentration of Type V cement.

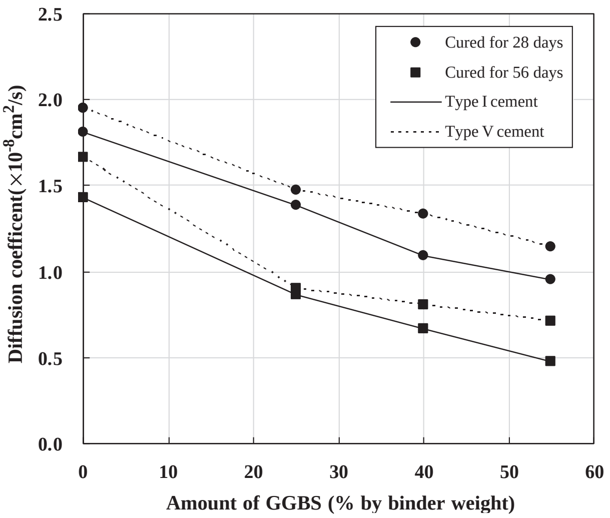

Fig. 9. The diffusion coefficient of chloride-ions in concrete containing GGBS.

3.4. Estimate of corrosion by half-cell potential test

Half-cell potential readings of specimens subjected to NaCl water-wetting and -drying cycles were recorded to compare the performances of the different concrete mixtures and to verify the surface areas of the corroded steel reinforcements. The half-cell potentials of the specimens (see Fig. 2) with 10 mm cover and 30 mm cover versus the repeated wetting–drying cycles of accelerating steel corrosion (see Fig. 3), up to 30 cycles, are illustrated in Fig. 10. The corrosion potentials of steel in GGBS concrete showed lower than −250 mV even before testing. The high corrosion potentials in the GGBS concrete specimens may be attributed to the reducing effects of sulfur species, such as S, SO2, S2O3, etc., derived from slag [24]. These sulfur species can reduce the potentials to much lower potentials depending on the concrete environment. The corrosion rate, however, remains low [25].

From a threshold value of −350 mV for steel bars embedded in the specimens, it can be supposed that the bars in the B4 mixture (Type I cement) rarely corroded and the reinforcements in B1 mixtures were corroded earlier than those in B4 mixtures. In B4 mixtures, the bars

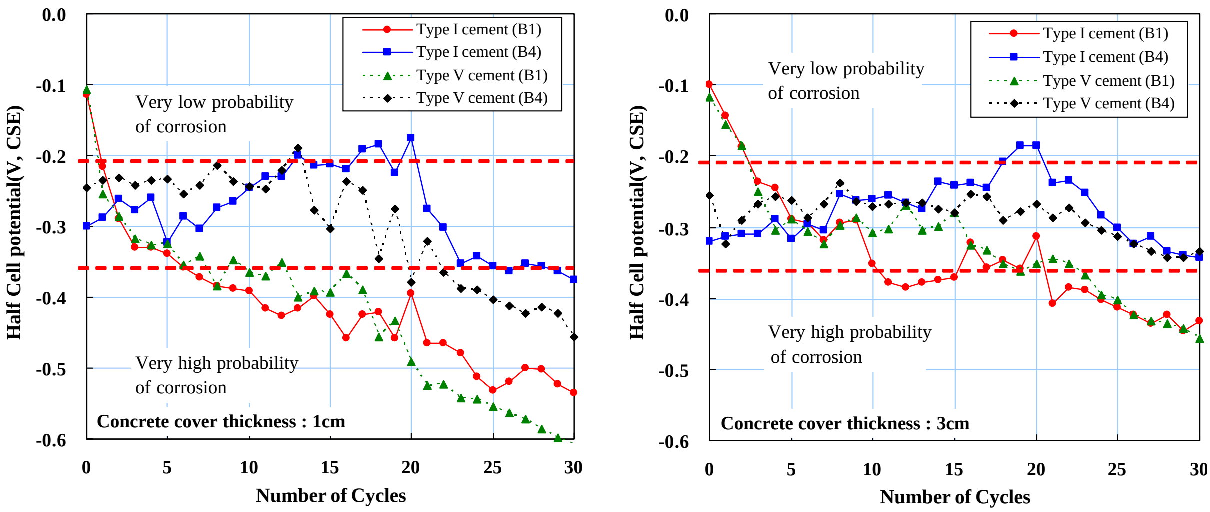

Fig. 10. Half-cell potentials.

embedded in Type I cement concrete started corroding later than that in Type V cement concrete. The results of the half-cell potential tests showed a tendency to decrease the potential readings as the number of cycles was increased. In accordance with ASTM C 876, all B1 concrete mixture specimens with concrete cover thickness of 10 mm indicated “very high probability over 90% of corrosion” before 10 cycles, but the B4 concrete mixture specimens exhibited “uncertain” before 20 cycles. This means that the B4 concrete mixture can reduce the probability of steel corrosion in concrete structure. In the case of all the specimens with 30 mm concrete cover, B4 mixtures (Types I and V cement) did not reach the potentials “very high probability over 90% of corrosion” at all cycles. Therefore, sufficient cover thickness and the proper cement type can delay salt attacks in an aggressive environment for the protection of ordinary reinforcements from corrosion.

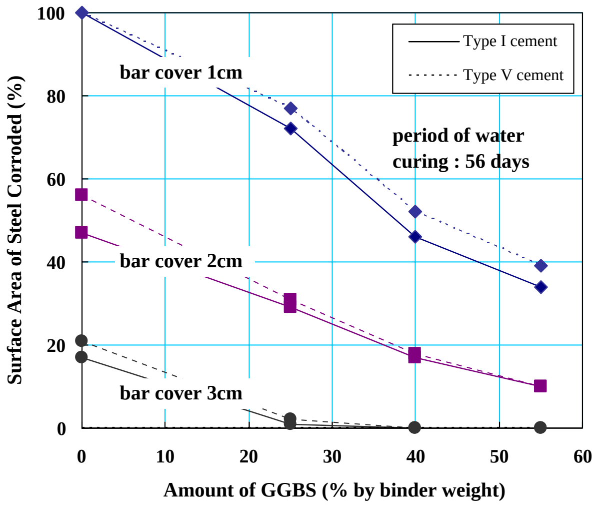

Fig. 11. Surface area (%) corroded from steel bars in concrete specimens.

3.5. Evaluation of the corroded surface areas of steel bars

As already mentioned, the HP test results depended on the environment of the tested concrete. In order to confirm the uncertainty of HP test results, it is important to check the corrosion rate of steel bars embedded in concrete specimens. Fig. 11 presents the test results obtained from the measurements of the surface area corroded from steel bars after concrete specimens were cured for 56 days in water and then the accelerated corrosion tests were carried out by 30 wetting–drying cycles (see Fig. 3). The results showed that the corroded surface area (%) depended on the thickness of the concrete cover, as well as the amount of GGBS mixed, and it is in accordance with the measurements of the half-cell potential test. The corroded areas of steel embedded in B1 concrete mixtures were about 2 times and 3 times larger than those of steel involved in B3 concrete mixture and B4 concrete mixture, respectively. Upon comparison of the corroded surface areas, the proportion of corroded areas in Type I cement was lower than that of the corroded areas in Type V cement. These results suggest that the resistance to steel corrosion can be superior, since not only was Type I cement used, but also the amount of GGBS was increased. It is also proposed that Type I cement can be replaced with 40% GGBS or more in order to increase the corrosion resistance of steel bars and decrease the probability of steel corrosion.

4. Summary and conclusions

Chloride resistance is the most important characteristic that prevents the premature deterioration of concrete structures. A comprehensive experimental study has been conducted to evaluate the influence of GGBS mixture proportions of concrete on the resistance to chloride permeability, chloride diffusion, and steel corrosion. The major test variables include amount of GGBS in mixture and type of cement. The principal findings can be drawn from the comprehensive test results as follows:

(1) The compressive strength of all compressive specimens exceeded design strength of 35 MPa before 28 days. Although GGBS mixture specimens showed lower compressive strength than B1 mixture ones at the early age, the compressive strengths of GGBS mixtures were stronger than that of B1 mixture after 28 days. These results came from the fact that secondary chemical reactions, latent hydraulicity reactions, attributed to make the microstructure of concrete specimens denser.
(2) Based on RCP test results, chloride-ion permeability of GGBS concrete specimens is reduced as period of curing or amount of GGBS by binder weight was increased. The permeability of Type I cement blended with GGBS was lower than that of Type V cement.
(3) ACID test results obtained from the cumulative increase of chloride-ion concentration indicate that much longer transition periods and much lower chloride-ion concentration can be achieved, if higher volumes of GGBS are added. The chloride-ion concentrations of Type I cement are lower than that of Type V cement, compared for the same amount of GGBS.
(4) Diffusion coefficients were decreased as the amount of GGBS or the period of curing was increased. It was in accordance with the measurements of RCP and ACID test. Type I cement showed lower diffusion coefficient compared to Type V cement.
(5) Corrosion potentials of steel in GGBS concrete specimens showed lower than about -250 mV even before testing because of the reducing effects of sulfur species, such as S, SO_2, S_2O_3, etc., derived from slag. The corrosion rate, however, remains low. Results of HP tests showed a tendency to decrease corrosion potential readings according to the increase of cycle, thickness of concrete cover, and GGBS content. Therefore, sufficient concrete cover thickness and proper cement type can delay chloride-ion attacks in an aggressive environment for the protection of ordinary reinforcement from corrosion.
(6) Surface area of steel corroded was depending on the thickness of concrete cover as well as the amount of GGBS mixed. The corroded areas of steel embedded in B1 mixture concrete specimens were about 2 times and 3 times larger than those of steel involved in B3 mixture concrete ones and B4 mixture concrete ones, respectively. The proportion of corroded area in Type I cement showed lower than that of the corroded area in Type V cement.
(7) Corrosion rate is deeply depending on the depth of concrete cover, cement type, and GGBS content. The resistance of steel corrosion is superior when the thickness of concrete cover is thick and high GGBS is blended with Type I cements rather than Type V cement. Type I cement concrete with GGBS of 40% or more by binder weight can increase the corrosion resistance of a steel bar more than two times, compared to GGBS-free cement concrete.

References

[1] A.A. Ramezanianpour, Effect of curing on the compressive strength, resistance to chloride-ion penetration and porosity of concretes incorporation slag, fly ash or silica fume, Cem. Concr. Compos. 17 (1995) 125–133.

[2] G.J. Osborne, Durability of portland blast-furnace slag cement concrete, Cem. Concr. Compos. 21 (1999) 11–21.

[3] E.F. Irassar, M. Gonzalez, V. Rahhal, Sulphate resistance of type V cements with limestone filler and natural pozzolana, Cem. Concr. Compos. 22 (2000) 361–368.

[4] K.M.A. Hossain, M. Lachemi, Corrosion resistance and chloride diffusivity of volcanic ash blended cement mortar, Cem. Concr. Res. 34 (4) (2004) 695–702.

[5] O.E. GjΦrv, Effect of condensed silica fume on steel corrosion in concrete, ACI Mater. J. 92-M60 (1995) 591–598.

[6] K. Torii, T. Sasatani, M. Kawamura, Effects of fly ash, blast furnace slag, and silica fume on resistance of mortar to calcium chloride attack, Proceedings of Fifth International Conference on Fly Ash, Silica Fume, Slag, and Natural Pozzolans in Concrete, American Concrete Institute, SP-153, vol. 2, 1995, pp. 931–949.

[7] T.M. El Sokkary, H.H. Assal, A.M. Kandeel, Effect of silica fume or granulated slag on sulphate attack of ordinary portland and alumina cement blend, Ceram. Int. 30 (2004) 133–138.

[8] A.K. Suryavanshi, J.D. Scantlebury, S.B. Lyon, The binding of chloride ions by sulphate resistant portland cement, Cem. Concr. Res. 25 (3) (1995) 581–592.

[9] S.E. Hussain, Rasheeduzzafar, A. Al-Musallam, A.S. Al-Gahtani, Factors affecting threshold chloride for reinforcement corrosion in concrete, Cem. Concr. Res. 25 (7) (1995) 1543–1555.

[10] X. Rasheeduzzafar, S.S. Al-Saadoun, A.S. Al-Gahtani, F.H. Dakhil, Effect of tricalcium aluminate content of cement on corrosion of reinforcing steel in concrete, Cem. Concr. Res. 20 (1990) 723–738.

[11] A.K. Suryavanshi, J.D. Scantlebury, S.B. Lyon, Corrosion of reinforcement steel embedded in high water–cement ratio concrete contaminated with chloride, Cem. Concr. Compos. (20) (1998) 263–381.

[12] H.A.F. Dehwah, M. Maslehuddin, S.A. Austin, Long-term effect of sulfate ions and associated cation type on chloride-induced reinforcement corrosion in Portland cement concretes, Cem. Concr. Compos. 24 (2002) 17–25.

[13] ASTM C 494, Standard specification for chemical admixtures for concrete, Annual Book of ASTM Standards, American Society for Testing and Materials, 1999.

[14] ASTM C 1202, Standard Test method for electrical indication of concrete's ability to resist chloride ion penetration, Annual Book of ASTM Standards, American Society for Testing and Materials, 1997.

[15] P.F. McGrath, R.D. Hooton, Influence of voltage on chloride diffusion coefficients from chloride migration tests, Cem. Concr. Res. 26 (8) (1996) 1239–1244.

[16] R.K. Dhir, M.R. Jones, H.E. Ahmed, A.M. Seneveratune, Rapid estimation of chloride diffusion coefficient in concrete, Mag. Concr. Res. 42 (152) (1990) 177–185.

[17] T. Sugiyama, S. Nagaoka, Y. Tsuji, C. Hashimoto, Electrical potential technique for determination of chloride diffusion coefficient of concrete, Proc. Jpn. Concr. Inst. 18 (1) (1996) 981–986.

[18] G.C. Kostogloudis, D. Kalogridis, C. Ftikos, C. Malami, B. Georgali, V. Kaloidas, Comparative investigation of corrosion resistance of steel reinforcement in alinite and portland cement mortars, Cem. Concr. Res. 28 (7) (1998) 995–1010.

[19] ASTM C 876, Standard test method for half-cell potentials of uncoated reinforcing steel in concrete, Annual Book of ASTM Standards, American Society for Testing and Materials, 1991.

[20] S.E. Hussain, Mechanisms of high durability performance plane and blended cements, PhD Dissertation, Department Civil Engineering, King Fahd University of Petroleum and Minerals, Dhahran, Saudi Arabia, 1991.

[21] A. Kumar, Della M. Roy, The effect of desiccation on the porosity and pore structure of freeze dried hardened portland cement and slag-blended pastes, Cem. Concr. Res. 16 (1986) 74–78.

[22] Rasheeduzzafar, S. Ehtesham Hussain, S.S. Al-Saadoun, Effect of tricalcium aluminate content of cement on chloride binding and corrosion of reinforcing steel in concrete, ACI Mater. J. 89 (1) (1999) 3–12.

[23] A.K. Suryavanshi, J.D. Scantlebury, S.B. Lyon, The binding of chloride ions by sulphate resistant Portland cement, Cem. Concr. Res. 25 (3) (1995) 581–592.

[24] D.E. Macphee, H.T. Cao, Theoretical description of impact of blast furnace slag (BFS) on steel passivation in concrete, Mag. Concr. Res. 45 (162) (1993) 63–69.

[25] O.S.B. Al-Amouid, Rasheeduzzafar, M. Maslehuddin, S.N. Abdul-jauwad, Influence of sulfate ions on chloride-induced reinforcement corrosion in Portland and blended cement concrete, Cem. Concr. Aggreg. 16 (1) (1994) 3–11.